NUMERICAL INVESTIGATION OF TURBULENT FLOW IN A TWIN RECTANGULAR SUB-CHANNEL GEOMETRY

D. Home[1,2], M. F. Lightstone[1] and M. S. Hamed[1,2]
[1] Department of Mechanical Engineering, McMaster University,[2] Thermal Processing Laboratory (TPL)
McMaster University, Hamilton, Ontario, Canada

Abstract

This abstract provides a summary of work-in-progress on using the Detached Eddy Simulation (DES) based turbulence modeling to investigate inter sub-channel thermal mixing. The effect of coherent vortical structures formed in the gap regions of sub-channel geometries was studied numerically. The study was performed on twin rectangular sub-channel geometry at a bulk Reynolds number of 2.15×10^3 with two different mesh structures. It was found that the code could correctly predict the qualitative effects of the flow pulsation phenomena on the turbulent flow field. The effect of numerical scheme on the performance of the DES model was studied as well.

1. Introduction

Mathematical modeling of turbulent mixing in a nuclear fuel rod bundle of a nuclear reactor core is of direct relevance to nuclear reactor safety analysis. CANDU nuclear reactor fuel assembly consist of a parallel matrix of solid rods, containing a fissile material and arranged in a pressure tube. Coolant flows along the rods to remove the heat generated by nuclear fission. The rod bundle contains a number of parallel sub-channels that are defined as small geometrical regions surrounded by rod surfaces and separated by hypothetical lines connecting the centroids of fuel rods. Sub-channels are bounded by either the fuel rod walls, pressure tube walls, or the region between the sub-channels referred to as 'gaps' as shown in Figure 1. Mass, momentum, and heat transfer between adjacent sub-channels occur mainly by turbulent transport, referred to as 'inter sub-channel mixing'. Accurate prediction of detailed temperature distribution in rod bundles both under normal operating conditions and under scenarios of accidents such as loss-of-coolant accident (LOCA) is essential for their safe design and reliable operation. A highly accurate prediction requires a detailed knowledge of the three dimensional velocity field in the rod bundle and a good understanding of the mixing process between interconnected sub-channels. The rod bundle thermal-hydraulics analysis is performed by solving the conservation equations for mass, momentum and energy. In the nuclear industry, the usual methods employed are sub-channel analysis, porous body model analysis, and distributed parameter analysis [1]. The basic limitation of the sub-channel and porous body methods is that they invoke a lumped parameter approach, where many empirical correlations are used to represent the complex exchange mechanisms between the sub-channels and thus do not calculate the fine structures of the velocity and temperature within the control volumes. Averaged mass flow rates and temperatures are computed within the individual control volumes. The interaction between the sub-channels is considered by means of mixing coefficients. Distributed parameter analysis [2] which is based on turbulence modeling is by far the most advanced design model and is undergoing rapid development. This approach is computationally costly and relies heavily on the empirical information of the turbulent transport properties of momentum and energy. Detailed experimental data is required for the velocity, temperature, and turbulence for modeling and code validation.

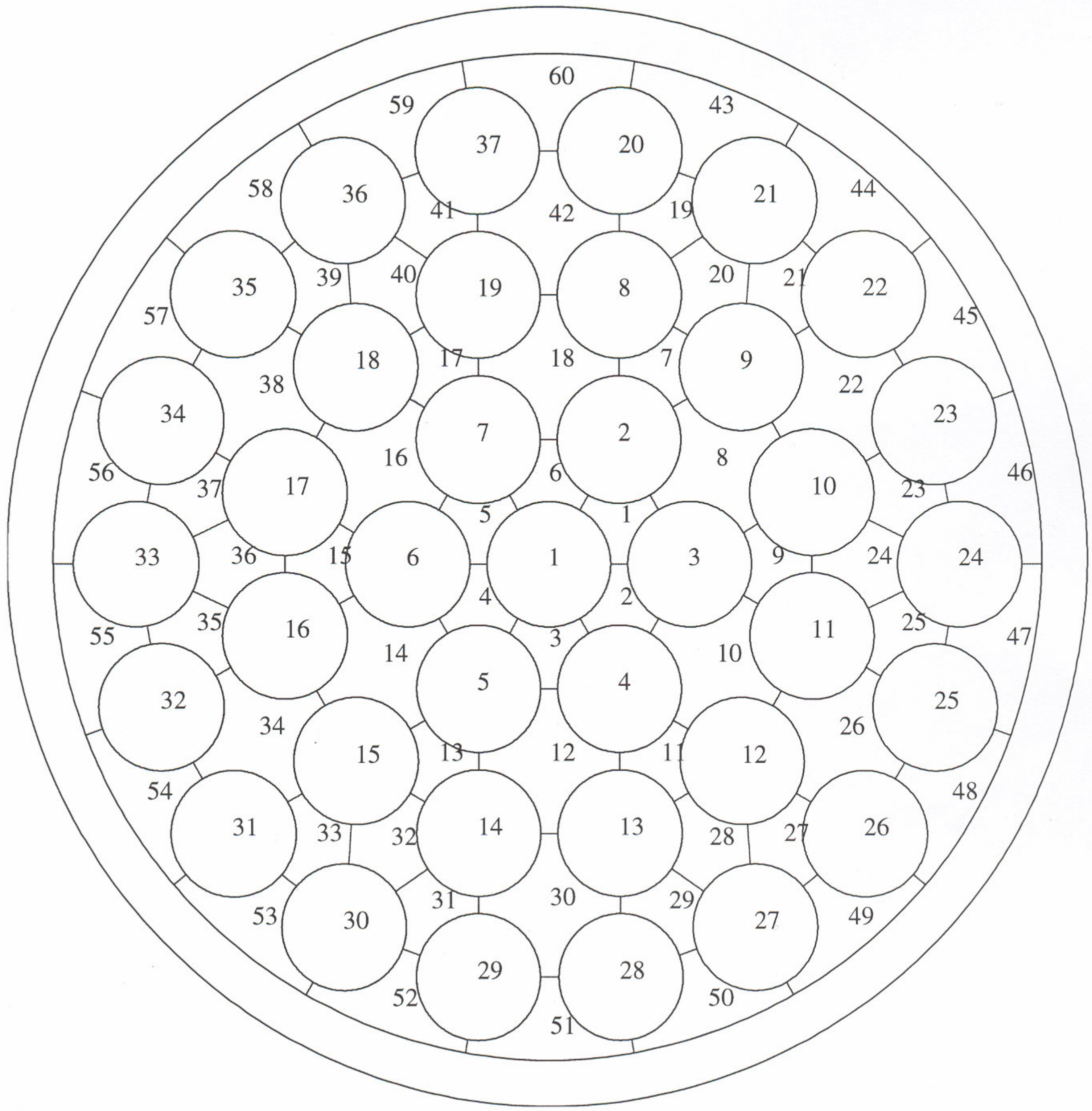

Figure 1 Cross section of a CANDU fuel bundle, showing different types of sub-channels.

For single-phase conditions, three different mechanisms contribute to the overall mixing process, namely, turbulent diffusion, convection by secondary flows, and large-scale eddy motion. Secondary flows in rod bundle geometry have proved to be very difficult to measure. In fact, some of the earliest attempts to measure secondary flows were not successful [3, 4]. Seale measured secondary flows in a duct simulating rod bundle arrangement. Seale, from his experimental and numerical investigations in a parallel sub-channel duct, concluded that secondary flows are insignificant for the high mixing rates observed experimentally [5, 6, 7]. Vonka reported experimental data on secondary flows in a central sub-channel of a triangular array [8]. He found that the magnitude of the secondary flow velocity is less than 0.1% of the axial velocity. The general conclusion is that secondary flows in rod bundle geometries are very small. They do not contribute significantly to the mixing between sub-channels of the rod bundles for small gap-to-diameter ratio, since secondary flow vortices are expected to move within the elementary cells of the sub-channels.

Experimental investigations have conclusively shown that cross sub-channel mixing is greatly enhanced by transport due to large-scale, quasi-periodic pulsations, which form across the gap. Moller performed an experimental study to investigate the macroscopic flow pulsations in rod bundle geometries with different aspect ratios [9]. Hot wires and microphones were used for the measurements of velocity and wall pressure fluctuations. He found peaks at characteristic frequencies in the power spectra of the turbulent velocity fluctuations in the axial direction and in the direction parallel to the walls. The frequency varied linearly with Reynolds number. Guelloz and Tavoularis did a comprehensive study of the structure of turbulent flow in a rectangular channel containing a cylindrical rod, focusing on the gap between the rod and the plane wall [10]. Reynolds-averaged and phase-averaged measurements were performed to characterize the features of the large-scale structures. The presence of large-scale, quasi-periodic structures in the vicinity of the gap, for a range of gap widths was demonstrated through flow visualization, spectral analysis and space-time correlation measurements. The measurements identified the large-scale structures with the field of a street of three-dimensional, counter rotating vortices, whose convection speed and stream-wise spacing were found to be functions of the gap width. The large-scale coherent structures are found to exist in any longitudinal slot or groove in a wall or a connecting gap between two flow channels, provided certain geometrical conditions are satisfied. The large eddies move almost periodically through the gaps of rod bundles at the characteristic frequency and are the main reason for the high mixing rates between sub-channels.

Conventional turbulence modeling approach like Reynolds Averaged Navier-Stokes (RANS) methods, based on the gradient transport mechanism have been grossly inadequate to predict the velocity and temperature fields accurately in rod bundle geometries, leading to inaccurate prediction of cross sub-channel mixing [11, 12]. From the numerical investigations performed till date, it is clear that unsteady turbulence models that can account for the quasi-periodic flow pulsations are required for accurate prediction of sub-channel mixing. Large eddy simulation (LES) would be a suitable method to approach the sub-channel mixing problem. LES has been successfully used for predicting turbulent flows around bluff bodies, which are dominated by large scale turbulent structures. Accurate results have been obtained for these flows using LES at an affordable cost. In contrast, wall bounded flows are a challenge for LES because of the fine grids required in the near wall region. While the cost of using LES to resolve energy carrying scales of motion away from the wall region does not depend strongly on the Reynolds number itself [13], if the near-wall region of a boundary layer needs to be resolved, the number of grid points required strongly depends on the Reynolds number. Thus, if the wall layer is completely resolved with LES, the computational costs are staggering and becoming almost comparable to a Direct Numerical Simulation (DNS). Methods have been developed to bypass the wall layer so as to perform high Reynolds number LES at a reasonable cost [14]. One such method is the Detached Eddy Simulation (DES) approach proposed by Spalart et al. [15], where a single grid is used and only the turbulence model changes. DES is a hybrid approach that combines the solutions of the Unsteady Reynolds Averaged Navier-Stokes (URANS) equations in the attached boundary layer, with LES in the separated regions in which the detached eddies are important. DES is a non-zonal technique, since it uses a single grid. The LES region is demarcated from the RANS region through the model used to calculate the turbulent eddy viscosity. In the near-wall region (URANS region) the effect of turbulent structures is modeled and in the outer region (LES region) the usual LES is used. In this way the requirement of high near-wall resolution is eliminated and wall bounded flows can be simulated at a more reasonable computational cost. In the original formulation of the DES, Spalart et al. [15] used the Spalart and Allmaras [16] model, a one-equation model in which a transport equation for the eddy viscosity is solved. This one-equation model is used both as a RANS model and sub-grid scale eddy viscosity model in the LES region. Another DES formulation is based on the model proposed by Strelets [17]. DES has also been tested thoroughly for problems without boundary layer separation such as turbulent channel flows [18, 19]. The present study of turbulent flow in a twin rectangular sub-channel geometry [20] is part of a long term research goal. The long term research aims at developing a better fundamental understanding of the nature and origin of large-scale quasi-periodic structures that are found in the gap regions of tightly packed rod bundle geometries, like the CANDU 37 fuel rod bundle. It is of interest to numerically identify the presence of large-scale coherent structures in rod bundles and their effects on the turbulence structure and heat transfer characteristics. The main objective of the research work is to develop a physics based constitutive model for inter sub-channel thermal mixing that could be implemented in a nuclear reactor thermal hydraulics code. Numerical identification of these structures is possible using inherently unsteady turbulence modeling approaches like DES or LES that resolve the large scale turbulence fluctuations. It was proposed that DES be used since it can be performed at a much lower computational cost as compared to LES.

The paper is organized as follows: in the next section, the DES model of Strelets [17] is presented. The twin sub-channel flow set up is discussed in the section on CFD methodology, which is followed by the results and conclusion section.

2. Strelets DES-SST model

The DES model of Strelets [17] uses the Shear Stress Transport (SST) model of Menter [21] to provide the eddy viscosity in the URANS region and the sub-grid scale viscosity in the LES region. The SST model which solves for the turbulence kinetic energy (k) and turbulence eddy frequency (ω) is a hybrid model, where a k-ω formulation is used in the near wall region, and a k-ε (ε is the dissipation rate of turbulent kinetic energy) formulation in the outer part of the boundary layer. For computations to be performed with one set of equations, the k-ε model is first transformed into a k-ω formulation. The blending between the two regions is performed by using a blending function F_1 that is designed to be unity in the near wall region, activating the k-ω model, and zero away from the surface, activating the k-ε model. The corresponding equations of the SST model are:

$$\partial_t(\rho k)+\partial_{x_j}(\rho U_j k)=P_k-\beta^*\rho\omega k+\partial_{x_j}\left[(\mu+\sigma_k\mu_t)\partial_{x_j}(k)\right] \tag{1}$$

$$\partial_t(\rho\omega)+\partial_{x_j}(\rho U_j\omega)=\gamma P_\omega-\beta\rho\omega^2+2\rho(1-F_1)\sigma_{\omega 2}\frac{1}{\omega}\partial_{x_j}(k)\partial_{x_j}(\omega)+\partial_{x_j}\left[(\mu+\sigma_\omega\mu_t)\partial_{x_j}(\omega)\right] \tag{2}$$

where $\beta^* = 0.09$ is the constant present in both the k-ω and the transformed k-ε model, $\sigma_{\omega 2} = 0.856$ is the constant present in the transformed k-ε model; σ_k, γ, β, σ_ω are the constants of the SST model which are a combination of constants from the k-ω and the transformed k-ε model. The eddy viscosity of the model is based on the assumption that the shear stress in a boundary layer is proportional to the turbulent kinetic energy. The eddy viscosity is given as:

$$\nu_t=\frac{a_1 k}{\max(a_1\omega;\Omega F_2)} \tag{3}$$

where a_1=0.31 is a constant, Ω is the absolute value of vorticity and F_2 is a blending function which behaves exactly like the blending function F_1. The formulations of the blending functions can be found in [21]. Turbulence models like SST that are based on the ω equation provide an analytical expression for ω in the viscous sub-layer. This allows for a near-wall formulation which gradually and automatically switches from wall functions to a low-Reynolds number near-wall formulation, as the grid is refined in the wall-normal direction.

The idea behind the DES model of Strelets [17] is to switch from the SST-RANS model to an LES model in regions where the turbulent length scale predicted by the RANS model is larger than the local grid spacing. In this case, the length scale used in the computation of the dissipation rate in the equation for turbulent kinetic energy is replaced by the local grid spacing. This is achieved by multiplying the destruction term of the turbulent kinetic energy equation with a switching function, i.e.

$$\varepsilon = \beta^* k\omega F_{DES} \tag{4}$$

where F_{DES} is the switching function that switches the SST-RANS model to an LES model. The formulation of F_{DES} is given as:

$$F_{DES} = \max\left(\frac{\sqrt{k}}{\beta^* \omega C_{DES}\Delta}, 1\right) \tag{5}$$

where Δ is the maximum local grid spacing in any direction, C_{DES} is a constant and equal to 0.61.

3. CFD methodology

The simulations were performed on the computational domain shown in Figure 2, using the DES-SST model available in ANSYS CFX-11.0. On this domain, experiments were conducted [20], so it provides a perfect test case to assess the validity of the turbulence model. The stream-wise, wall-normal and span-wise directions are indicated by x, y and z respectively. The velocity components (in brackets) in the respective directions are also shown in Figure 1. The bulk (mean) flow was in the stream-wise direction. The Reynolds number, Re_{Dh} based on the hydraulic diameter and the mean flow velocity was 2.15×10^3. Table 1 provides the geometrical details for the cross-section of the domain. Based on the information provided in the experiments, on the stream-wise spacing between the large-scale structures formed near the gap, the length of the domain was set to 730 mm so as to capture three vortices each of two alternating sequences. Simulations were performed for three different cases. Cases C1 and C2 were performed on the same mesh which had a total number of nodes of 633,850, whereas, case C3 had a much finer mesh using a total grid points of 1,560,900. For the mesh with 633,850 grid points, 50 nodes were used in the stream-wise direction. The gap cross-section was modeled with 9 (wall-normal) × 25 (span-wise) grid points. Uniform meshing law was applied in all the three directions. For the fine mesh (1,560,900 grid points), 100 nodes were used in the stream-wise direction, and the gap was modeled with 9 (wall-normal) × 43 (span-wise) grid points. Uniform meshing law was used for the stream-wise direction, whereas, for the wall-normal and span-wise an expanding grid was used, with the growth ratio between the cells of about 1.03. In this case the aspect ratio of the cells varied from 2 to 746 and was an overly refined mesh. The two different meshes are shown in Figures 3 and 4 respectively.

The code in ANSYS CFX uses finite volume discretization, with fully implicit time advancement scheme. For the present computations, in all cases, the time discretization was carried out using the

Second-Order Backward Euler Scheme. For all the equations (continuity, momentum and turbulence) in the LES region, the advection scheme used by the code is the Second-Order Central Difference Scheme, which reduces the effect of numerical dissipation. However, in the URANS region, either the Upwind (First-Order or Second-Order) or the Second-Order Central Difference Scheme can be used as the advection scheme. When the solver advection scheme is set as Upwind, the code uses an Upwind scheme in the URANS region which automatically changes to a Central Difference scheme once the DES model switches to LES. A Central Difference scheme is used throughout the domain, when the solver advection scheme is set as Central Difference. For case C1, the advection scheme in the URANS region was Second-Order Central Difference. For cases C2 and C3, in the URANS region, the advection scheme for the continuity and momentum equations was Second-Order Upwind and for the turbulence equations it was First-Order Upwind (based on CFX discretization theory guidelines).Thus the effect of the numerical treatment of the advection scheme was studied between cases C1 and C2.

In the simulations, periodic boundary condition was applied in the stream-wise direction. Mass flow rate was specified in the stream-wise direction to drive the flow. Wall boundary condition was specified in the remaining two directions. The initial velocity field for the DES run was specified from a steady SST run. The code has the ability to superimpose specified velocity fluctuations on the initial velocity field to "kick start" the process, and this was used. The time step used in the simulations was based on the frequency of the flow pulsation phenomena observed in the experiment [20]. For cases C1 and C2, the time step was 10^{-4} sec and $CFL_{max}<1$, whereas for case C3, it was 10^{-5} sec (because of a highly refined mesh) and $CFL_{max}\leq 6$. The time step used for cases C1 and C2 was suitable for the simulations to be run for sufficiently long time to be statistically independent of the initial condition; however for case C3 this could not be insured. In all cases, the simulation was run till 5000 time steps, from where statistics like mean velocity, velocity correlations, and Reynolds stresses were accumulated for another 5000 time steps.

4. Results and discussion

As indicated in Figure 2, time history of the flow variables was monitored at points 1 (centre of the gap), 2, 3 (edge of the gap) and 4. The coordinates of these points were obtained from the experiment [20]. The instantaneous velocity, U, in any direction, is a combination of its time averaged value, $\overline{U}$, and the fluctuating component, u. In the discussion of results, all turbulence variables are non-dimensionalized using the average wall friction velocity. The turbulence variables are denoted as: k (resolved turbulence kinetic energy), u' (stream-wise turbulence intensity), v' (wall-normal turbulence intensity), w' (span-wise turbulence intensity), $\overline{uv}$ and $\overline{uw}$ (Reynolds shear stresses). A typical contour of the time averaged axial velocity (normalized by the bulk velocity) as predicted by the DES model is shown in Figure 5. It is clear, that the cross flow through the gap causes the velocity contour to bulge, which was also seen in the experiments [20]. The bulging is more pronounced near the gap region. The presence of secondary flows causes the velocity contour to bulge near the four corners of the duct. The velocity contour was found to have good symmetry with respect to the symmetry axis through the gap. The predicted velocity contour matched well with the experiment [20]. The predicted average wall friction velocity (u*) in comparison with the experiment [20] is provided in Table 2. In all cases, the DES model under predicts the wall shear stress, which is typical of DES simulations [18]. Table 3 provides the quantitative comparison between the DES simulations and the experiment [20], for the maximum values in the turbulence variables. The simulations were in excellent agreement with the experiment in detecting the location

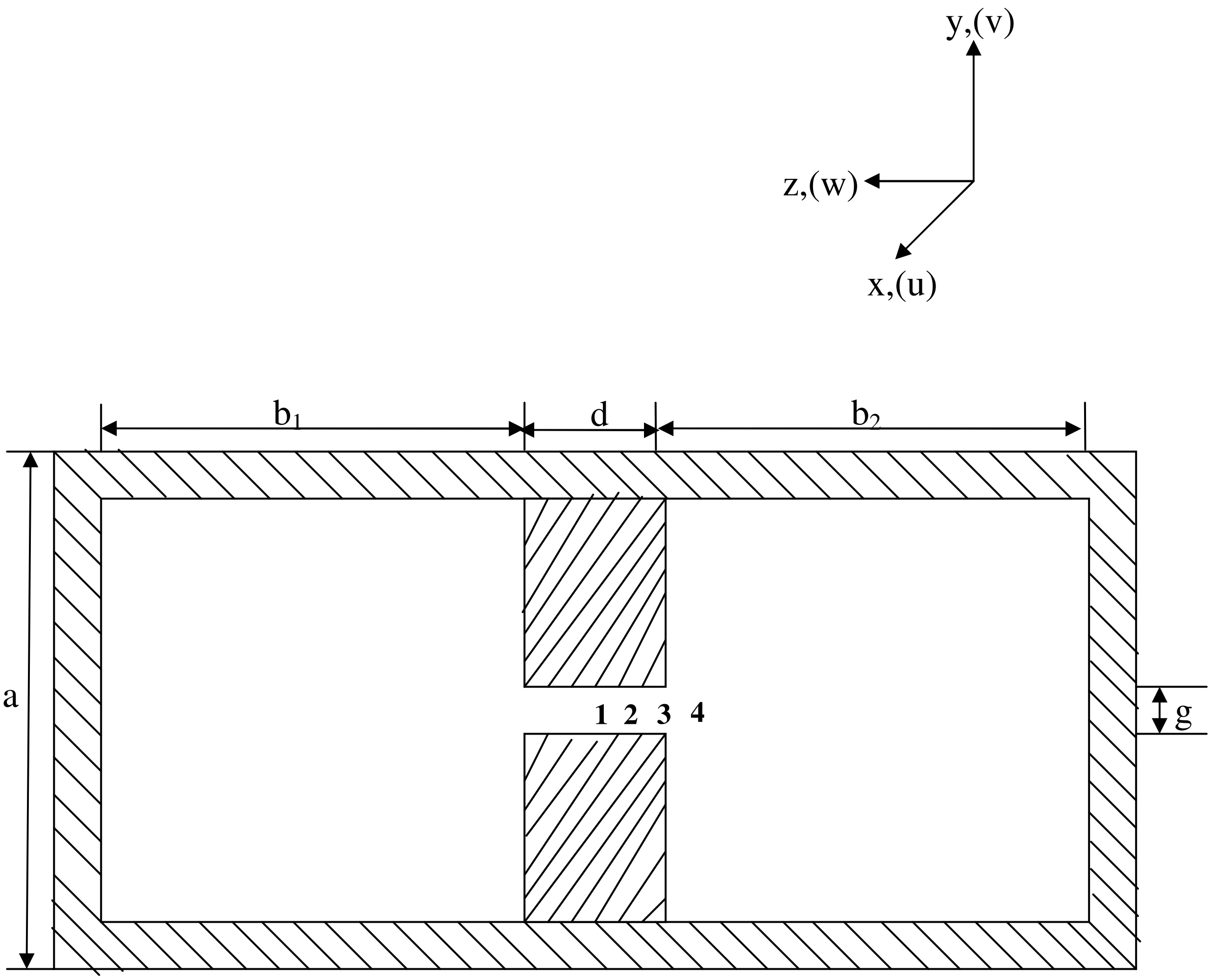

Figure 2 Cross-section and the coordinate axis of the twin rectangular sub-channel geometry.

Table 1 Geometrical details for the cross-section of the computational domain.

a (mm)	b_1(mm)	b_2(mm)	d(mm)	g(mm)
180.0	136.4	136.2	76.96	10.0

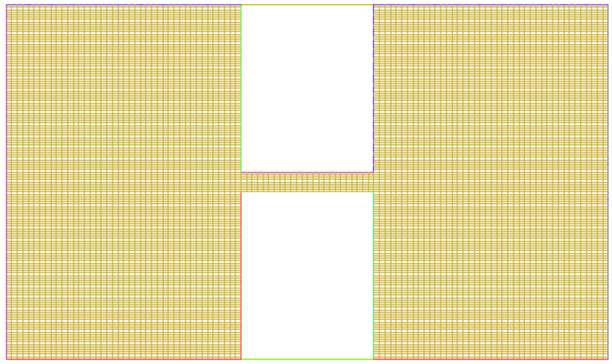

Figure 3 Mesh with 633,850 grid points.

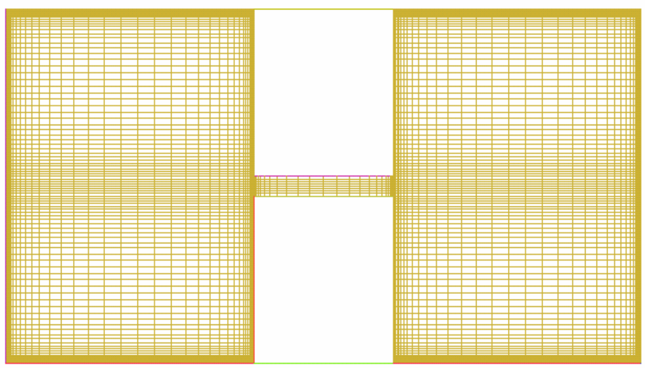

Figure 4 Mesh with 1,560,900 grid points.

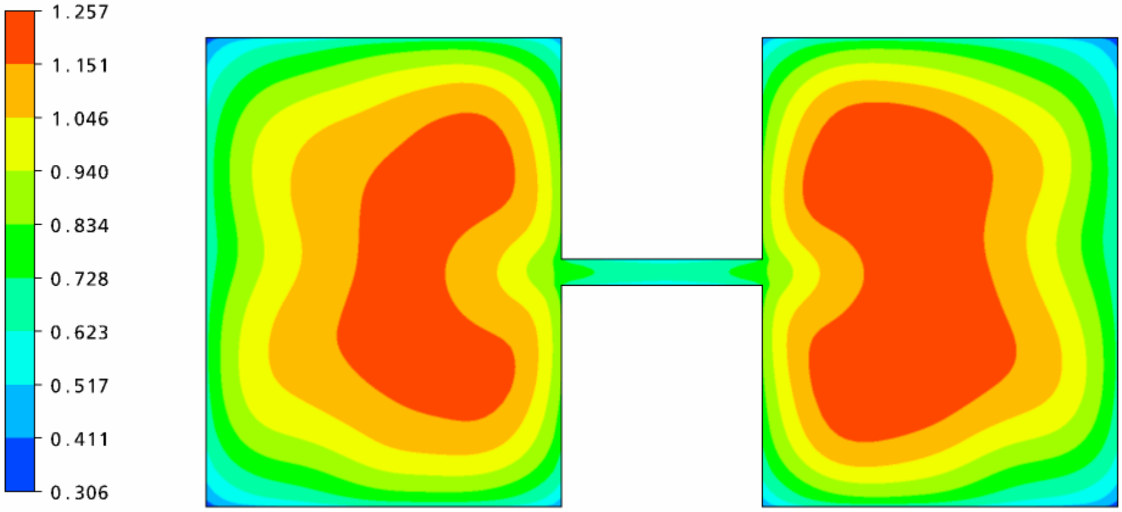

Figure 5 DES prediction of time averaged axial velocity (Case C1).

of the maximum values. It is evident from Table 3, that all the variables were over predicted. The differences between cases C1 and C2 were minimal, and this was expected. In general, the agreement for cases C1 and C2 with the experiment [20] was good. However, case C3 considerably over predicted the values, by almost a factor of 2. The reason for this (for case C3) could be the fact that the statistics were initiated much earlier and were accumulated for a short interval of simulation time. The small time step for case C3 was an impediment in terms of initiation and accumulation of statistics, hence statistically significant results were not achieved. Following are the qualitative observations on the turbulence variables from the DES predictions. The stream-wise turbulence intensity u', was found to have very large values near the edges of the gap. The turbulence intensity in the y-direction, was also very high near the vicinity of the gap. The intensity v' was found to have two peaks near the edges of the gap. The transverse intensity in z-direction (parallel to gap), was very high along the whole depth of the gap. The combined effect of all this is observed in the turbulence kinetic energy, for which a contour plot is shown in Figure 6. The turbulence kinetic energy is very high in the region close to the gap, and has two peaks at the corners of the gap. The peak value at the gap was much higher than the highest values at the other walls without a gap. The contour of the gap parallel Reynolds shear stress $\overline{uw}$ is shown in Figure 7. The shear stresses near the gap are much higher than anywhere else in the channel. In the gap region, the shear stress $\overline{uv}$ has two peaks, a positive and a negative one, whereas the shear stress $\overline{uw}$ has only one peak. The shear stress $\overline{uw}$ is zero at the symmetry line between the two channels at the centre of the gap. These results show that the flow in a twin rectangular sub-channel geometry is different from flow in a regular duct. The qualitative aspects of the flow were well predicted by the DES model and were in agreement with the experiment [20].

Table 2 Comparison of average wall friction velocity.

Case	u*(m/s)
C1	0.829
C2	0.829
C3	0.776
Experiment [20]	0.924

Table 3 Comparison of peak value in the turbulence variables.

Case	k	u'	v'	w'	$\overline{uv}$	$\overline{uw}$
C1	10.8	4.0	1.5	2.5	± 1.5	6.5
C2	9.4	3.9	1.2	2.2	± 1.4	5.7
C3	22.6	6.1	2.6	4.0	± 7.5	12.0
Experiment [20]	9.2	3.4	2.0	2.0	± 2.4	4.4

The time traces of the instantaneous span-wise velocity at the monitor point 1 (centre of the gap) is shown in Figures 8 and 9 respectively. Figure 8 shows the time trace for cases C1 and C2, whereas Figure 9 is the time trace for case C3. It is clear from both the figures, that there is significant velocity directed along the z-direction, which was also observed for other monitor points. This clearly suggests, that fluid pulsations occur across the width of the gap. In the experiment [20], the span-wise velocity at the monitor point 1 had a periodic nature with a well defined periodicity of around 68 Hz, which is a characteristic of sub-channel flows. However, Figure 8 does not show a periodic pattern in the time trace, it shows a pure turbulent nature in the flow. It was found for cases C1 and C2, that for the entire gap region, LES part of the DES model could not be triggered. Case C3 had a more refined mesh, and it was found that for the entire gap region LES was operating. Figure 9 does show presence of a periodic pattern in the flow, with a frequency of approximately 78 Hz. Cases C1 and C2 over predicted the velocity through the gap, however for case C3, limits of the velocity through the gap was in line with the experiment [20]. Table 4 and 5 provides the quantitative comparison between the simulations and the experiment [20], for the time averaged velocity and for different Reynolds stress components. Table 4 and 5 are flow data pertaining to monitor points 1 (gap centre) and 3 (gap edge) respectively. For the variable $\overline{U}$, cases C1 and C2 over predict at the gap centre and at the gap edge, whereas case C3 under predicts at the gap centre and predicts it quite well at the gap edge. Statistical Reynolds stress $\overline{uu}$ is over predicted by a factor of almost 2 to 5. The Reynolds stress $\overline{ww}$ is well predicted by cases C1 and C2, however case C3 over predicts by a factor of 2. DES predictions of the Reynolds shear stress $\overline{uw}$ show a different trend (in terms of sign) as compared to the experiment [20]. At the gap edge, the magnitude of $\overline{uw}$ is

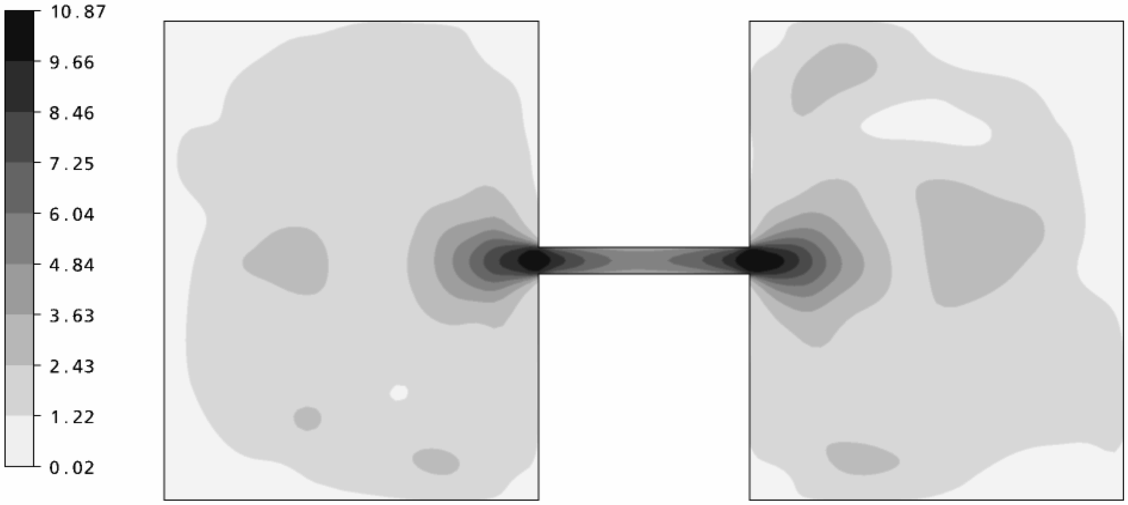

Figure 6 DES prediction of turbulence kinetic energy (Case C1).

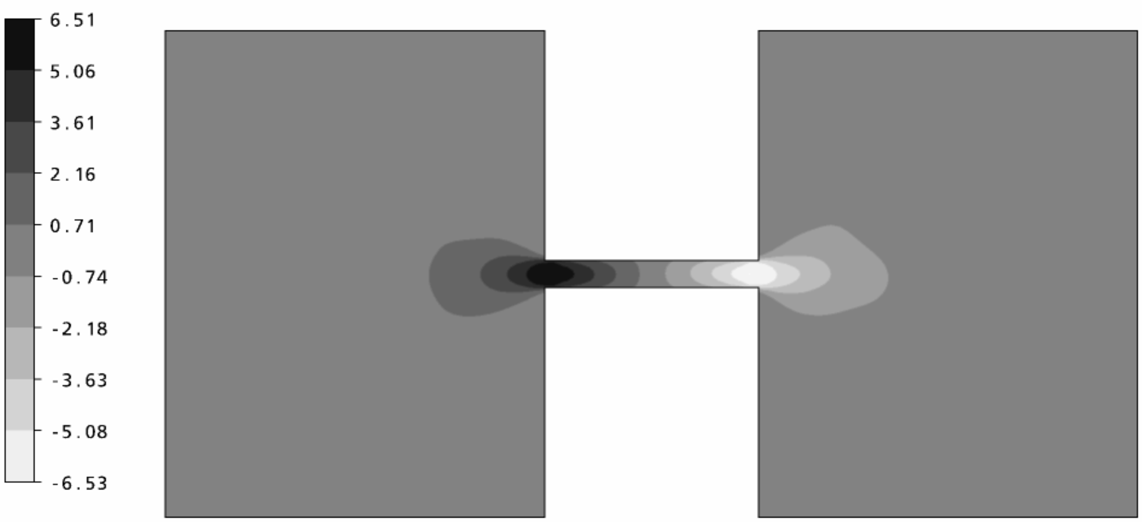

Figure 7 DES prediction of gap parallel Reynolds shear stress (Case C1).

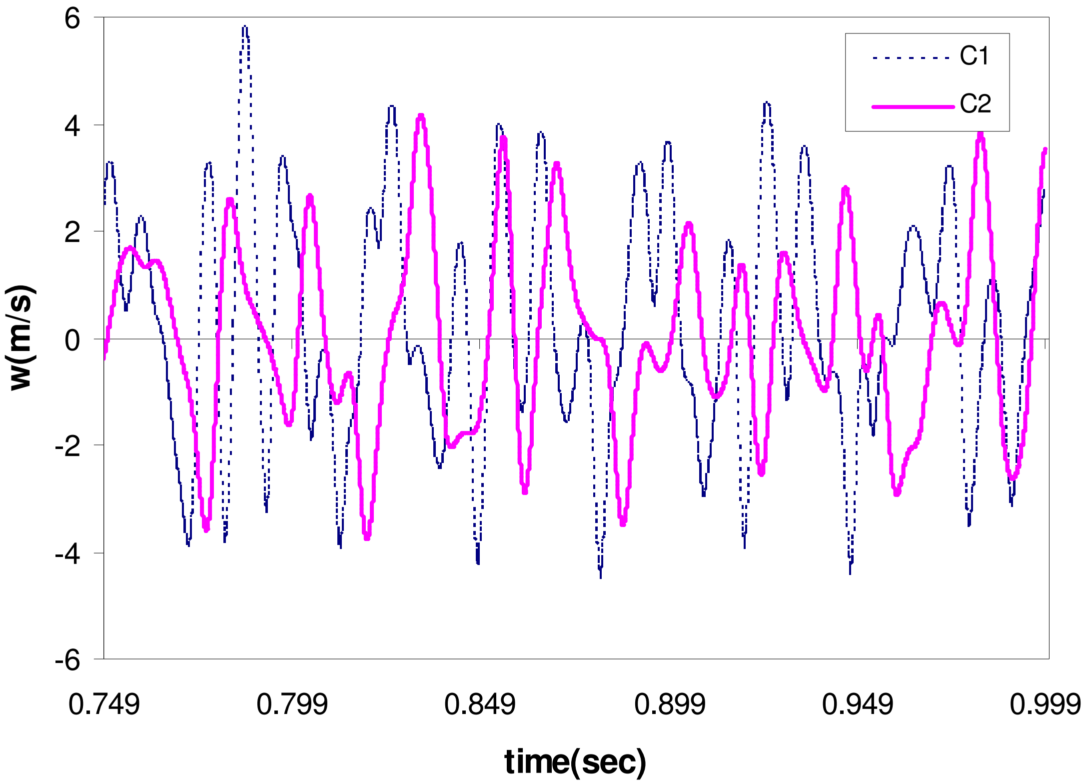

Figure 8 DES prediction of the time trace of span-wise velocity at the centre of the gap.

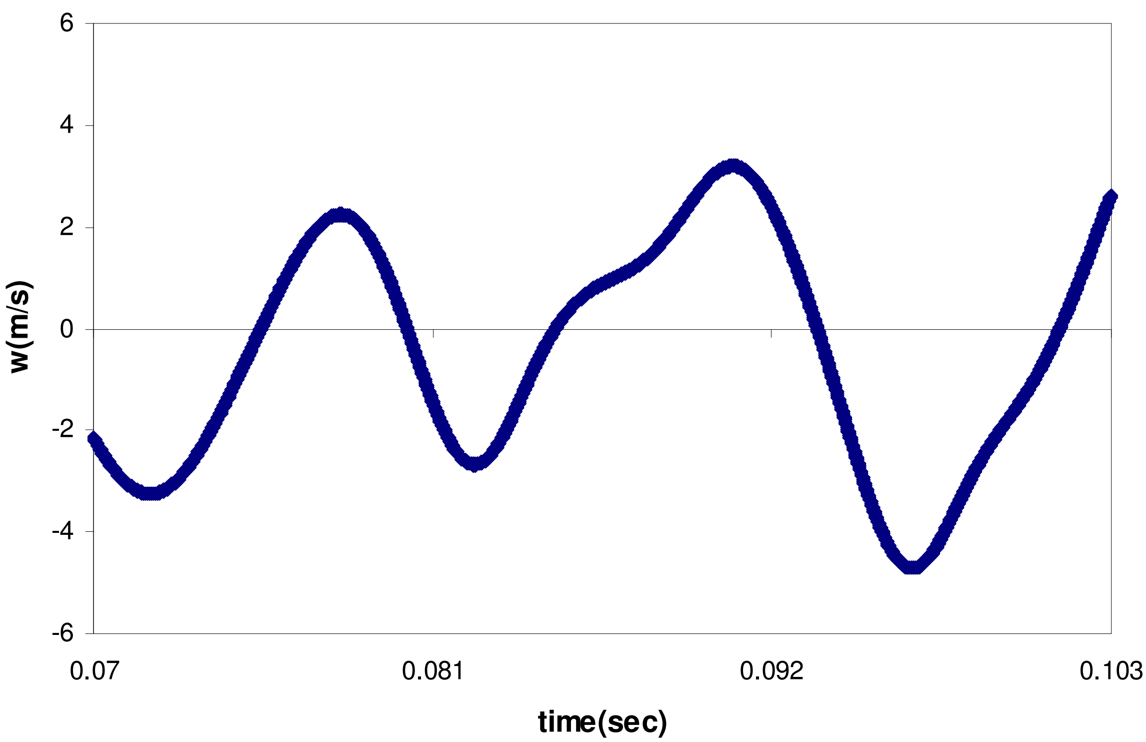

Figure 9 DES prediction of the time trace of span-wise velocity at the centre of the gap (C3).

well predicted by all the cases, however the sign is opposite. Case C2, predicts $\overline{uw}$ quite well at the gap centre, in terms of magnitude and sign. It is perhaps not appropriate to directly compare numerical data and the experimental result at specific points for the correlations involving cross velocity components, and the reason for this is not known at this stage. As stated before, differences between cases C1 and C2 were minor. The problem with case C3 was its small time step.

Table 4 Flow data pertaining to monitor point 1.

Case	$\overline{U}$ (m/s)	$\overline{uu}$ (m^2/s^2)	$\overline{ww}$ (m^2/s^2)	$\overline{uw}$ (m^2/s^2)
C1	14.04	3.586	3.868	0.088
C2	13.29	2.62	3.18	-0.17
C3	9.88	5.59	6.81	0.552
Experiment [20]	11.54	0.976	3.596	-0.172

Table 5 Flow data pertaining to monitor point 3.

Case	$\overline{U}$ (m/s)	$\overline{uu}$ (m^2/s^2)	$\overline{ww}$ (m^2/s^2)	$\overline{uw}$ (m^2/s^2)
C1	17.28	10.867	3.588	-4.308
C2	16.57	10.08	2.78	-3.85
C3	15.00	7.32	6.16	-4.21
Experiment [20]	14.73	4.938	3.061	3.095

Figure 10 shows the contour of the instantaneous span-wise velocity for case C3, in the plane parallel to the flow (x-z plane). It is clear that alternate sequence of positive and negative velocities are present, and are directed through the gap (z-direction). For this particular case, 4 alternating sequences were present. The presence of large-scale structures is evident from the contour. The patterns are not that well organized as what was expected. However, the simulations were successful in capturing the presence of large-scale vortices in the gap region. These large-scale structures are in the form of vortices, which have their centres on either side of the gap axis but within the gap. The vortices in the alternate sequences, rotate in opposite directions and are driven by the higher velocities outside the gap. Figure 11 shows the velocity vectors in the x-z plane. It is clear that the presence of alternate sequence of vortices causes the fluid to follow a zig-zag path in the entire gap region along the whole channel length. The strong peaks that are observed in the near gap region for the turbulence kinetic energy and the Reynolds shear stresses are a result of the vortical structures formed in the gap region. The turbulence kinetic energy is produced in the near gap region. The presence of these vortices causes the fluid to flow from one sub-channel to the other in an alternating fashion, which results in an effective inter sub-channel thermal mixing.

5. Conclusion

The DES simulations were successful in detecting the presence of large-scale structures in a twin rectangular sub-channel geometry. The simulations had a good qualitative agreement with the experiment [20]. All the essential features of the turbulence flow field in a sub-channel geometry were well captured. Present work is directed in creating an improved mesh structure which would have good quantitative agreement with the experiment [20]. Work is also directed in proposing a physical model which would explain the formation of the large-scale structures in the gap region.

6. Acknowledgment

The authors would like to acknowledge the financial support provided by University Network of Excellence in Nuclear Engineering (UNENE) and Natural Sciences and Engineering Research Council of Canada (NSERC).

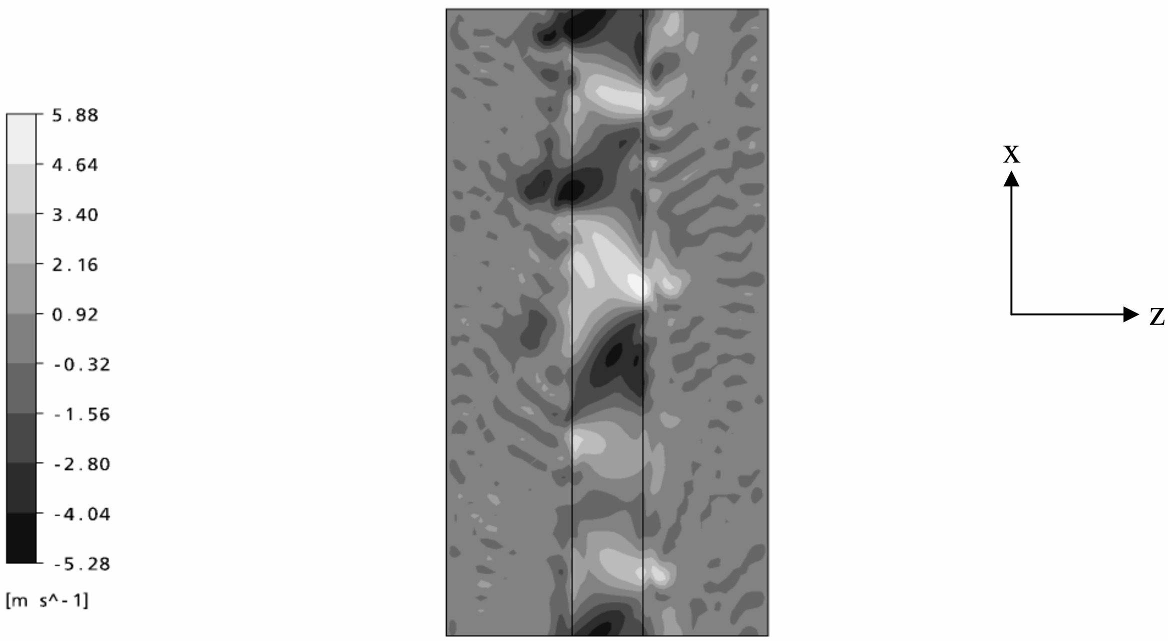

Figure 10 DES prediction of span-wise velocity (Case C3).

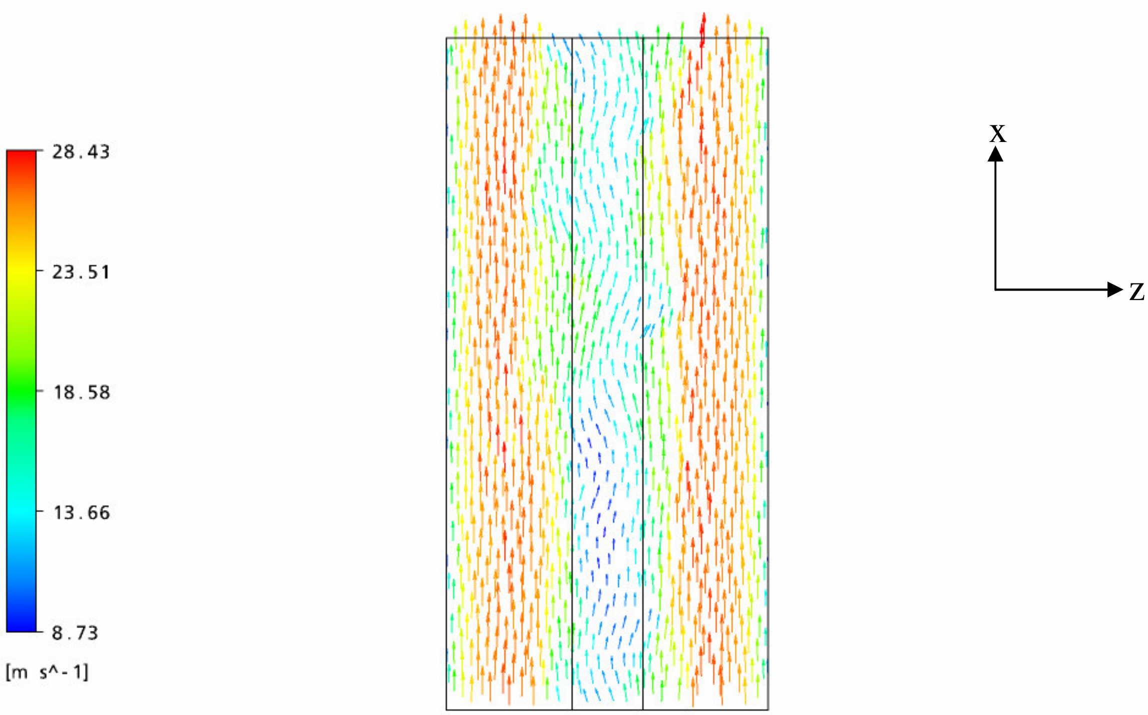

Figure 11 DES prediction of velocity vector (Case C3).

7. References

[1] Rehme K., ‘‘The structure of turbulence in rod bundles and the implications on natural mixing between the subchannels”, *International Journal of Heat and Mass Transfer*, Vol. 35, Iss. 2, 1992, pp.567-581.

[2] Rehme K., ‘‘The structure of turbulent flow through rod bundles”, *Nuclear Engineering and Design*, Vol. 99, 1987, pp.141-154.

[3] Trupp A.C., and Azad R.S., ‘‘The structure of turbulent flow in triangular array rod bundles”, *Nuclear Engineering and Design*, Vol. 32, 1975, pp.47-84.

[4] Carajilescov P., and Todreas N.E., ‘‘Experimental and analytical study of axial turbulent flows in an interior subchannel of a bare rod bundle”, *ASME Journal of Heat Transfer*, Vol. 98, 1976, pp.262-268.

[5] Seale W.J., ‘‘Turbulent diffusion of heat between connected flow passages, Part 1: Outline of problem and experimental investigation”, *Nuclear Engineering and Design*, Vol. 54, 1979 a, pp.183-195.

[6] Seale W.J., ‘‘Turbulent diffusion of heat between connected flow passages, Part 2: Predictions using the ‘‘k-ε’’ turbulence model”, *Nuclear Engineering and Design*, Vol. 54, 1979 b, pp.197-209.

[7] Seale W.J., ‘‘Measurements and predictions of fully developed turbulent flow in a simulated rod bundle”, *Journal of Fluid Mechanics*, Vol. 123, 1982, pp.399-423.

[8] Vonka V., ‘‘Measurement of secondary flow vortices in a rod bundle”, *Nuclear Engineering and Design*, Vol. 106, 1988, pp.191-207.

[9] Moller S.V., ‘‘Single-phase turbulent mixing in rod bundles”, *Experimental Thermal and Fluid Science*, Vol. 5, 1992, pp. 26-33.

[10] Guellouz M.S., and Tavoularis S., ‘‘The structure of turbulent flow in a rectangular channel containing a cylindrical rod - Part 1: Reynolds-averaged measurements”, *Experimental Thermal and Fluid Science*, Vol. 23, 2000, pp.59-73.

[11] Rock R.C.K., and Lightstone M.F., ‘‘A numerical investigation of turbulent interchange mixing of axial coolant flow in rod bundle geometries”, *Numerical Heat Transfer*, Vol. 40, 2001, pp.221-237.

[12] Suh Y.K., and Lightstone M.F., ‘‘Numerical simulation of turbulent flow and mixing in a rod bundle geometry”, *Nuclear Energy*, Vol. 43, Iss. 1, 2004, pp.1-11.

[13] Piomelli U., Balaras E., Pasinato H., Squires K.D., and Spalart P.R., ‘‘The inner-outer layer interface in large-eddy simulations with wall-layer models”, *International Journal of Heat and Fluid Flow*, Vol. 24, 2003, pp.538-550.

[14] Piomelli U., and Balaras E., ‘‘Wall-layer models for large-eddy simulations”, *Annual Review of Fluid Mechanics,* Vol. 34, 2002, pp.349-374.

[15] Spalart P.R., Jou W-H., Strelets M., and Allmaras S.R., ‘‘Comments on the feasibility of LES for wings, and on a hybrid RANS/LES approach”, First AFOSR International Conference on DNS/LES, Ruston, LA, 4-8, August, 1997, in Advances in DNS/LES, edited by C.Liu and Z.Liu (Greyden, Columbus, OH, 1997).

[16] Spalart P.R., and Allmaras S.R., ‘‘A one-equation turbulence model for aerodynamic flows”, 30th Aerospace Sciences Meeting & Exhibit, January 6-9, 1992 / Reno, NV.

[17] Strelets M., **‘‘**Detached eddy simulation of massively separated flows”, *AIAA Paper*, 2001-0879, 2001, pp.1-10.

[18] Nikitin N.V., Nicoud F., Wasistho B., Squires K.D., and Spalart P.R., ‘‘An approach to wall modeling in large-eddy simulations”, *Physics of Fluids*, Vol. 12, Iss. 7, 2000, pp.1629-1632.

[19] Home D., Lightstone M.F., and Hamed M.S., ''Detached Eddy Simulation based turbulence modeling approach for inter sub-channel thermal mixing", The 12th International Topical Meeting on Nuclear Reactor Thermal Hydraulics (NURETH-12), Sheraton Station Square, Pittsburgh, Pennsylvania, U.S.A., September 30-October 4, 2007.

[20] Meyer L. and Rehme K., ''Large-scale turbulence phenomena in compound rectangular channels", *Experimental Thermal and Fluid Science*, Vol. 8, 1994, pp. 286-304.

[21] Menter F.R., ''Improved two-equation $k-\omega$ turbulence models for aerodynamic flows", *NASA Technical Memorandum 103975*, 1992.